

Optimization of Air Route Network Nodes to Avoid "Three Areas" Based on An Adaptive Ant Colony Algorithm

Wang Shijin^{*}, Li Qingyun, Cao Xi, Li Haiyun

College of Civil Aviation, Nanjing University of Aeronautics and Astronautics, Nanjing 211106, P. R. China

(Received 22 August 2015; revised 16 November 2015; accepted 5 January 2016)

Abstract: Air route network (ARN) planning is an efficient way to alleviate civil aviation flight delays caused by increasing development and pressure for safe operation. Here, the ARN shortest path was taken as the objective function, and an air route network node (ARNN) optimization model was developed to circumvent the restrictions imposed by "three areas", also known as prohibited areas, restricted areas, and dangerous areas (PRDs), by creating a grid environment. And finally the objective function was solved by means of an adaptive ant colony algorithm (AACA). The A593, A470, B221, and G204 air routes in the busy ZSHA flight information region, where the airspace includes areas with different levels of PRDs, were taken as an example. Based on current flight patterns, a layout optimization of the ARNN was computed using this model and algorithm and successfully avoided PRDs. The optimized result reduced the total length of routes by 2.14% and the total cost by 9.875%.

Key words: air route network planning; three area avoidance; optimization of air route network node; adaptive ant colony algorithm; grid environment

CLC number: U8 **Document code:** A **Article ID:** 1005-1120(2016)04-0469-10

0 Introduction

In recent years, with the rapid development of aviation industry, sustained growth of air traffic has caused airspace congestion, flow control flight delays, and other problems more and more serious. The air route network (ARN), whose structure determines the operational efficiency of traffic flow and transportation costs, is the physical space where air traffic takes place. ARN planning is an effective way to allocate and use airspace resources rationally, eliminate airway bottlenecks, and ensure aviation safety.

Riviere achieved and improved global ARN optimization technology to attain the objective of minimum cost or distance, using a grid covering whole Europe and based on the no-sector concept proposed by Dudong^[1-2], as shown in Fig. 1. The operating characteristics of China's airspace control have led Chinese researchers to air route net-

work node (ARNN) local optimization technology to attain the objective of minimum cost of distance^[3-7] using optimization problem-solving thinking and intelligent optimization algorithms.

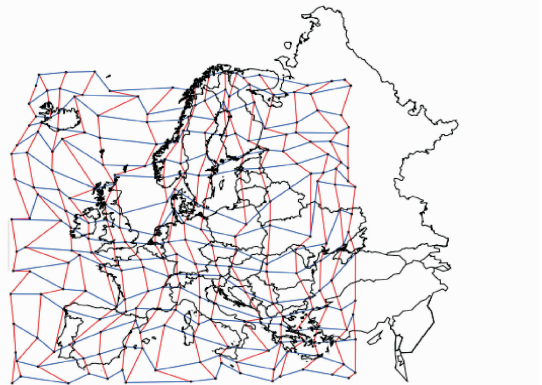


Fig. 1 Global planning grid overlay

However, the research has barely addressed the inevitable restrictions of the airspace structure in the process of ARN optimization. China's airspace contains many "three areas", also known as

^{*}Corresponding author, E-mail address: shijin_wang@nuaa.edu.cn.

the prohibited areas, restricted areas, and dangerous areas (PRDs), which are unavailable airspace for ARN optimization, and "fragment" the optimization environment exhibit, as shown in Fig. 2. Two studies have considered airspace environment restrictions in ARN optimization. On the one hand, the MAKLINK graph model proposed by Zhao and restricted by the number, shape, and layout of PRDs can avoid convex PRDs, but does not apply to concave PRDs, which severely limits its applicability^[8]. On the other hand, Wang successfully completed an ARN design while avoiding various PRD shapes by using cellular automata (CA), but this approach is restricted by the complexity of rule-making^[9], which reduces its overall efficiency.

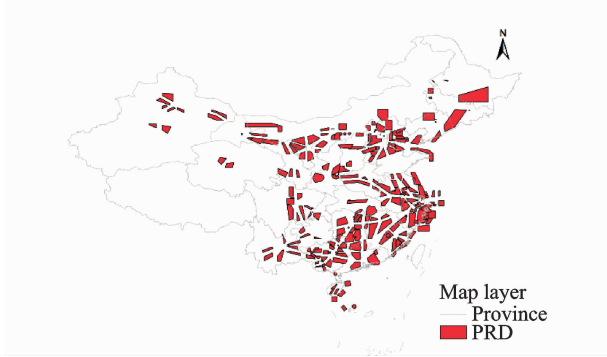


Fig. 2 ARN optimization "fragmented" environment

The concept of ground mobile robot path planning is to establish an abstract model of the path using a grid method^[10-12] and then to use a genetic algorithm (GA) to achieve obstacle avoidance and path planning in a position environment using binary coding. However, the length of code increases with the number of grid cells, leading to a high computational complexity. This method is applicable only to grid sizes of not more than 16×16 problems. To solve this problem, Zhang^[13-14] redefined the insert and delete operators. This method is simple, and its search ability is powerful, but the problem that the GA chromosome is too long is still not resolved. Zhang^[15] used the ant colony concept and chose the distance from the target and the pheromone concentration in the direction of motion as heuristic factors, an approach working well. However, this algorithm

takes a long time to search and easily stagnates.

In this context, improving solution efficiency while achieving spatial PRD avoidance would be very helpful. According to the relative positions of the current node and the destination node, an adaptive ant colony algorithm (AACA) combined with a certain selection probability and a random selection strategy in a grid environment was proposed. The AACA was used to solve the ARNN optimization model with a shortest-path objective function, avoiding PRD boundaries. Then five typical routes across different numbers of PRDs in the ZSHA airspace were selected as an example to verify the feasibility of the algorithm.

1 ARNN Optimization Model

1.1 Assumptions in ARNN optimization model

When building the ARNN optimization model (considering only the ARN, without the approach control area and terminal control area), the following assumptions were proposed:

- (1) Aircraft fly along the center line of the route;
- (2) ARN is a two-dimensional plane network which does not consider the climb or descent of aircraft;
- (3) Aircraft fly at a constant speed on the route and are uniformly distributed with equal spacing;
- (4) Aircraft arrive at and leave an intersection point in the same direction, and the intersecting tracks consist of plane linear segments;
- (5) PRDs cannot be traversed, but the PRD boundary mentioned earlier is the extended one, which belongs to the safety zone.

1.2 Establishment of ARNN optimization model

ARNN can be described as follows

$$N = (V, \mathbf{D}, U, \mathbf{C}, T, I, B) \quad (1)$$

where $V(N)$ is the set of ARNN. There are two kinds of nodes; Intersection points and airport points. n, m represent the number of intersection points and airports, respectively

$$V(N) = \{v_1, \dots, v_n, v_{n+1}, \dots, v_{n+m}\} \quad (2)$$

where the location of v_i is expressed by (x_i, y_i) ,

v_i represents an intersection point, if $i \leq n$, and an airport, if $n < i \leq n + m$.

$D(N)$ is a matrix of the segment lengths between pairs of nodes in the ARN.

$$D(N) = (d_{ij})_{(m+n) \times (m+n)} = \begin{bmatrix} d_{11} & \cdots & d_{1,m+n} \\ \vdots & \ddots & \vdots \\ d_{m+n,1} & \cdots & d_{m+n,m+n} \end{bmatrix} \quad (3)$$

where d_{ij} represents the linear distance between i and j

$$d_{ij} = \begin{cases} \sqrt{(x_i - x_j)^2 + (y_i - y_j)^2} & \text{if the segment is connected by } v_i \text{ and } v_j \\ 0 & \text{otherwise} \end{cases} \quad (4)$$

$U(N)$ means the segments connected by nodes (including the nodes) cannot be in $U(N)$, which can be described

$$\text{line}(i, j) \cap U(N) = \Phi \quad (5)$$

where Φ represents the empty set.

$C(N)$ means potential flight conflict risk probability of the set of intersection points

$$C(N) = (c_i)_{1 \times (m+n)} = \{c_1, \dots, c_m, \dots, c_{m+n}\} \quad (6)$$

where c_i reflects airspace safety and can be represented as

$$c_i = \sum_{j=1}^S \sum_{k=j+1}^{S-1} \left[\left(\frac{2f_{ji}f_{ki}}{X} \right) \cdot Y \cdot \arccos\left(\frac{\alpha_{jik}}{2}\right) / (f_{ji} + f_{ki}) \right] < c_{\max} \quad (7)$$

where c_i represents the hourly average potential flight conflict risk probability of ARNN nodes v_i ; f_{ji} and f_{ki} represent the flight flows of segment (v_j, v_i) and (v_k, v_i) , respectively; X represents the cruising speed (km/h); Y the lateral separation standard (km) under radar control; α_{jik} the intersection angle of segments (v_j, v_i) and (v_k, v_i) ; S the number of intersecting segments on v_i ; and c_{\max} the threshold value of the hourly average potential flight conflict risk probability of ARNN.

$T(N)$ is the total cost of flight paths, which can serve as a measure of ARN economy; the lower the total cost, the more economical the network is

$$T(N) = \sum_{i=1}^{n+m} \sum_{j=1}^{n+m} f_{ij} d_{ij} \leq T_{\max} \quad (8)$$

$I(N)$ is the nonlinear coefficient, defined as the ratio of the actual length and the linear length between ARNNs. The nonlinear coefficient of the network can be used to measure the convenience of the overall ARN; the larger its value, the higher the flight costs, and the lower the airspace utilization

$$I(N) = \frac{\sum_i^j d_{ij}}{G_{ij}} \leq i_{\max} \quad (9)$$

where d_{ij} and G_{ij} represent the actual length and the linear length, respectively, between two nodes i, j .

$B(N)$ is the boundary constraint of ARNNs. The significance of this constraint is that ARNNs must be located in the planning area

$$x_{\min}^i \leq x_i \leq x_{\max}^i, \quad y_{\min}^i \leq y_i \leq y_{\max}^i \quad (10)$$

where x_i and y_i represent the coordinates of v_i , x_{\min}^i and x_{\max}^i the lateral limits of v_i , and y_{\min}^i and y_{\max}^i the longitudinal limits of v_i .

The ARNN optimization mathematical model can be described by Eqs. (11)–(14). Eq. (11) is the shortest-path objective function; Eqs. (12)–(14) are constraints; Eq. (12) is the PRD restriction on the segments to optimize; Eq. (13) maintains the safety level of the intersection points; and Eq. (14) limits the boundary to the planned ARN

$$\min D = \sum_{i=1}^{n+m} \sum_{j=1}^{n+m} d_{ij} \quad i \geq j \quad (11)$$

$$\text{s. t.} \quad \text{line}(i, j) \cap U(N) = \emptyset \quad (12)$$

$$c_i < c_{\max} \quad (13)$$

$$x_{\min}^i \leq x_i \leq x_{\max}^i, y_{\min}^i \leq y_i \leq y_{\max}^i \quad (14)$$

2 Solvement ARNN Optimization Model

2.1 Establishing ARN grid environment

The grid method is used to divide the ARN airspace into a regular and uniform grid. The grid is divided into two states: An obstacle grid and a free grid. Fig. 3, for example, establishes an 8×9 grid environment and specifies the left bottom

corner as the coordinate origin. Using the lateral direction as the x -axis and the longitudinal direction as the y -axis, a rectangular coordinate system is established. Now set PRDs and the flight corridor as an obstacle grid (black grid) and a free grid (represented by grid numbers), respectively. PRD accounts for one or more of the grid cells; if it is less than one grid cell, the incomplete cell is regarded as a complete grid cell. There are at least two free grid cells between disjoint obstacle grid cells. The location of the start and the end points can be anywhere in a free grid, but the aircraft can move only one step to an adjacent grid cell.

All grid cells are identified using a combination of a serial numbering method and the rectangular coordinate system.

(1) Serial numbering method

Starting from the lower left corner of the grid in Fig. 3, all grid cells are numbered from left to right and from top to bottom. The serial number n ranges from 1 to 72. An identified grid cell is referred to as g_n . The grid cell with serial number 1 is referred to as g_1 , as shown in Fig. 3.

	y								
	1	2	3	4	5	6	7	8	9
	10	11	12	13	14	15	16	17	18
	19	20	21	22	23	24	25	26	27
	13	14	15	31	32			35	36
	37	38		40	41			44	45
	46	47	48	49	50	51	52	53	54
	55	56	57	58	59	60	61	62	63
	64	65	66		68	69	70	71	72
	0								x

Fig. 3 Relations between grid coordinates and serial numbers

(2) Rectangular coordinate method

The grid geometric center of the rectangular coordinates is defined as the grid coordinates $g(x, y)$. The serial number 1 of the grid cell in Fig. 3 is $g(0.5, 0.5)$.

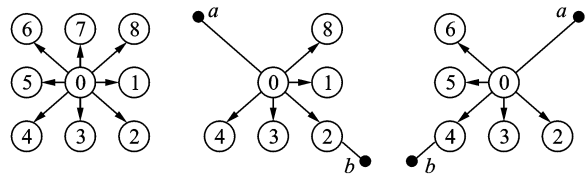
The correspondence between the coordinates and the serial numbers of a grid cell is given

$$\begin{aligned}
 x &= \text{mod}(i - 1, N_x) + 0.5 \\
 y &= \text{fix}((i - 1) / N_x) + 0.5
 \end{aligned}
 \tag{15}$$

where N_x is the serial number of the lateral grid cell, mod is a remainder operation to solve, and fix is a discard remainder rounding operation.

2.2 Adaptive ant colony algorithm

A traditional ant colony algorithm (ACA) search pattern can be used to solve the problem of two-dimensional ARN planning. As shown in Fig. 4(a), the aircraft is located in the center grid cell 0, and the remaining eight adjacent grid cells are transferable grid cells (excluding obstacle grid cells and grid cells already traversed). This search pattern takes much time, and it is easy to encounter singular segments.



(a) Transferable grid (b) $k < 0$ search pattern (c) $k > 0$ search pattern

Fig. 4 Search pattern

The AACA was proposed in this paper with a selection strategy which combined deterministic selection and probabilistic random selection. On the one hand, deterministic selection determines the search strategy according to the relative positions of the optimized nodes. Assume that the direction of the search path is from a to b . Regardless of vertical and horizontal special cases, the relative positions of ARNN fall into two cases: the slope between two nodes $k < 0$ (as shown in Fig. 4(b)) and $k > 0$ (Fig. 4(c)). Further, assume that the aircraft is located at grid cell 0, which belongs to segment ab . The aircraft flies from a to b , and only the adjacent five grid cells 1, 2, 3, 4, and 8 (excluding obstacle grid cells and grid cells already traversed) are passed through. If $k < 0$, the algorithm proceeds in a similar manner. The aircraft flies from a to b , and only the adjacent five grid cells 2, 3, 4, 5, and 6 (excluding obstacle grid cells and grid cells already traversed) need to be searched if $k > 0$. If the "ants" do not have a subsequent grid cell to choose, they can be seen as having fallen into a

trap, and an "ant fallback strategy" is used to ensure that they reach their destination safely. On the other hand, probabilistic random selection refers to the use of a "roulette wheel" to select the next grid cell and dynamically adjust the deterministic choice probabilities during the search process.

The direction of search is ensured to reduce the number of search grid cells and singular segments. For example, international route A593 passes through two PRDs. According to Section 2.1, a 50×50 array was built in MATLAB in the form of a grid environment, as shown in Fig. 5. Black and white grid cells represent PRDs and free flight areas, respectively. Traditional ACA was then used to search the neighboring eight directions for the optimal route. The broken line in Fig. 5 (a) represents the initial route, the solid line the optimal route as obtained by traditional ACA, and the segments in circles indicate

obvious singular segments and redundant ARNN nodes after optimization. Aircraft do not fly in singular segments. The dotted line in Fig. 5 (b) indicates the initial optimal route, which has reduced the large number of singular segments using the AACA.

2.3 Process of solving the optimization model

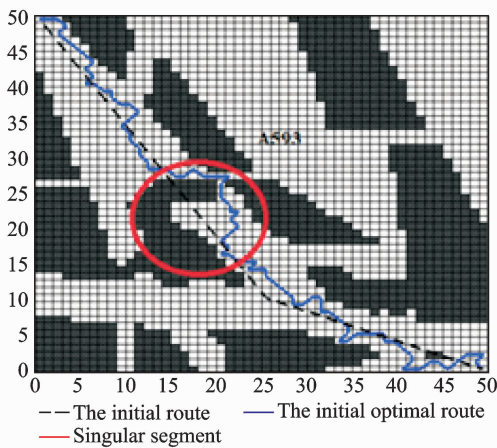
According to Section 2.1, a grid environment is established. The steps to solve the ARNN optimization model using AACA under the grid environment are as follows.

Step 1 According to the structure of the airspace to optimize, the geographical position and the grid position, which are represented by the M pairs of starting and target nodes of the segment to optimize, are confirmed. The positional relation and search pattern of the M pairs of nodes are also confirmed.

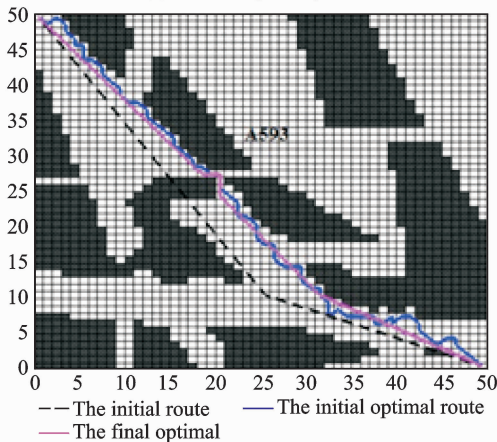
Step 2 The data and the ant taboo table are initialized. The initial pheromone of the path to optimize is set to a constant value, the number of ants to m , and the number of iterations to N . m ants are then placed into the grid at the starting node, and the initial position of each ant enters the ant taboo table.

Step 3 When the aircraft transfers, it is necessary to determine whether it has a selectable grid cell available. If not, the ant has fallen into a trap and must be removed from the simulation. Otherwise the "roulette" method is used to select the next grid cell where the aircraft can transfer. According to state transition of Eq. (16), the probability of the next selected grid cell is calculated and its transition probabilities are used as a cumulative probability, generating a random number. If the random number falls into the scope of one cumulative probability, the corresponding cumulative probability grid cell will be the following grid cell. This process is iterated until the destination grid cell is reached. Any ant that does not reach the destination grid cell are removed from the simulation.

$$p_{ij}(t) = \begin{cases} \frac{[\tau_{ij}(t)]^\alpha [\eta_{ij}(t)]^\beta}{\sum [\tau_{ij}(t)]^\alpha [\eta_{ij}(t)]^\beta} & j \in \text{allowed}_k \\ 0 & \text{Otherwise} \end{cases} \tag{16}$$



(a) ARN diagram by ACA



(b) ARN diagram by AACA

Fig. 5 ARN diagram by two algorithms

where α is a factor representing the elicitation of information, β the desired heuristic factor, $\tau_{ij}(t)$ the intensity of pheromone track (i, j) at time t ; the heuristic function η_{ij} is equal to $1/d_j$; and d_j is the distance between the grid cell which can be chosen for transfer and the end of the grid, directing the ants search routes toward destination node.

Step 4 The taboo table and the recorded path are updated. The grid cell passed through in the ARN is added to the ant taboo table. The distance between the grid cell where the ant is located and the east, the south, the west, and the north adjacent grid cells is 1. The distance between the grid cell where the ant is located and the southeast, the southwest, the northwest, and the northeast adjacent grid cells is $\sqrt{2}$. Each route and its length between the start and the destination of ARNN are recorded for all remaining ants.

Step 5 The paths of all the remaining ants that reach the destination grid cell are revised. Curved paths between adjacent grid cells are straightened, and the total path length is reduced as much as possible. According to Eqs. (17)–(19), the pheromones on the paths which the remaining ants have traversed are updated

$$\tau_{ij}(t+n) = (1-\rho) \cdot \tau_{ij}(t) + \Delta\tau_{ij}(t) \quad (17)$$

$$\Delta\tau_{ij}(t) = \sum_{k=1}^M \Delta\tau_{ij}^k(t) \quad (18)$$

$$\Delta\tau_{ij}^k = \begin{cases} \frac{Q}{L_k} & \text{If pass through path } (i, j) \\ 0 & \text{Otherwise} \end{cases} \quad (19)$$

where $\Delta\tau_{ij}$ is the amount of pheromone per unit length of trail that ant k leaves on edge (i, j) ; $1-\rho$ the pheromone residual factor; L_k the path length of ant k in the search; and Q the intensity of the pheromone.

Step 6 After iteration, the shortest path between each pair of nodes is output. By increasing the number of grid cells, the optimal path will be more precise. The final optimal ARN is then formed.

Step 7 The constraints of the optimal final

ARN are checked. According to the method in Ref. [16], the security level of ARNNs is verified. The optimal final ARN is then output. Otherwise, according to the severity and possible consequences of unsafe times or conditions, nodes $c_i \geq c_{\max} = 1 \times 10^{-3}$ may be re-optimized.

3 Case Study

The national air routes and PRDs were visualized using ArcGIS, as shown in Fig. 6. The term "line" refers to an upper air route, and an irregular "block" represents a PRD. The area outlined in bold lines is ZSHA. The density of air routes and PRDs shows that ZSHA is a typical busy airspace in China. ZSHA includes Jinan, Qingdao, Hefei, Shanghai, Xiamen, and Nan-chang, six upper control areas, and 20 control sectors. It contains 11 dangerous airspaces and 55 restricted airspaces, including more PRDs than any other flight information region (FIR) in China. With the development of civil aviation, rapid growth of air traffic has led to a series of problems, such as ARN airspace congestion and flight delays.

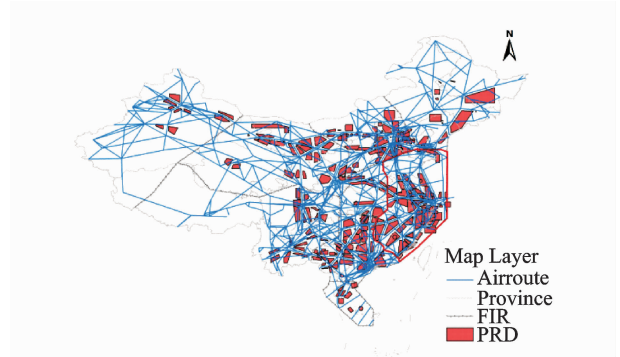


Fig. 6 ZSHA location of schematic diagram

Four representative international routes, G204, A470, B221, and A593 in ZSHA, were selected. Using MATLAB simulation platform, AACA was used to establish, solve, and verify the feasibility of the ARNN model in ZSHA based on the grid environment. Finally, the ArcGIS software was used to visualize the results before and after optimization, as shown in Fig. 7, where

the block sections represent PRDs; The solid line and the dotted line the initial route and the optimal routes respectively; the hollow rim and the solid rim represent the initial ARNN and the optimal ARNN respectively. The coding was marked as those in Ref. [17]. The numbers from 1 to 21 indicate the nodes traversed by the routes to be optimized. G204, A470, B221, and A593 passed three, two, three, and two PRDs.

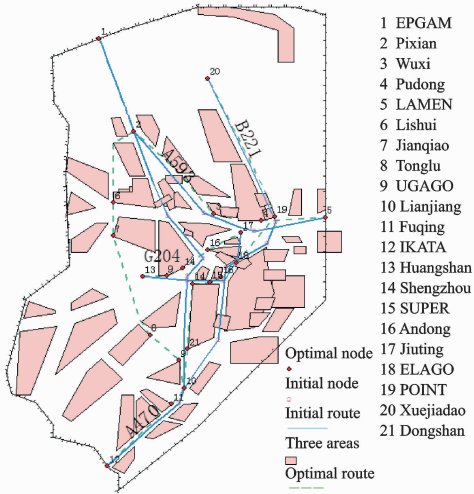


Fig. 7 Comparison of ARN before and after optimization

According to Part 2 (establishment of the optimization model) and Part 3 (solving the algorithm), the ARNN optimization process includes basic data, the optimization model, and solving the three modules, as shown in Fig. 8.

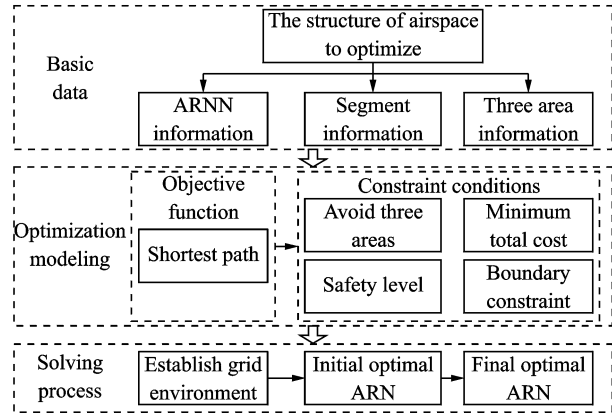


Fig. 8 Module chart of ARNN optimization

The basic data module in Fig. 8 includes collection and pretreatment of basic data. It analyzes the airspace status quo in ZSHA and confirms the number and location of PRDs, segments, and ARNNs to optimize the ZSHA network, as shown in Table 1. According to airport informa-

Table 1 Comparison of node coordinates between before and after optimization

No.	Node Name	Original node coordinate	Present node coordinate	No.	Node Name	Original node coordinate	Present node coordinate
1	EPGAM	N 37 14 48 E 116 52 59	N 37 14 48 E 116 52 59	12	IKATA	N 23 45 54 E 117 08 10	N 23 45 54 E 117 08 10
2	Pixian	N 34 18 42 E 117 58 37	N 34 18 42 E 117 58 37	13	Huangshan	N 29 44 14 E 118 15 16	N 29 44 14 E 118 15 16
3	Wuxi	N 31 44 30.3 E 120 11 25.4	N 31 43 08.4 E 120 29 56.4	14	Shengzhou	N 29 35 56.8 E 120 48 54	N 29 30 14.4 E 119 48 46.8
4	Pudong	N 31 10 14.2 E 121 46 57	N 31 30 10.8 E 121 59 56.4	15	SUPER	N 30 01 23 E 120 51 29	N 29 43 22.8 E 120 43 40.8
5	LAMEN	N 31 36 36 E 124 00 00	N 31 36 36 E 124 00 00	16	Andong	N 30 15 18.2 E 121 13 14	N 30 34 51.6 E 120 18 18
6	Lishui	N 31 39 01 E 119 02 25	N 32 04 12 E 117 19 51.6	17	Jiuting	N 31 07 20.9 E 121 20 27	N 31 07 20.9 E 121 20 27
7	Jianqiao	N 30 18 13.5 E 120 09 57	N 28 20 09.6 E 118 10 51.6	18	ELAGO	N 30 48 00 E 122 11 00	N 30 10 44.4 E 121 12 46.8
8	Tonglu	N 29 45 55 E 119 39 39	N27 53 16.8 E 118 29 09.6	19	PINOT	N 31 27 00 E 122 27 00	N 31 37 37.2 E 122 24 54
9	UGAGO	N 29 37 39 E 119 39 08	N 27 05 52.8 E 119 24 00	20	Xuejiangdao	N 120 17 9.6 E 35 58 53.88	N 120 17 9.6 E 35 58 53.88
10	Lianjiang	N 26 13 16 E 119 32 57	N 26 13 16 E 119 32 57	21	Dongshan	N 27 44 56 E 120 37 42	N 27 27 07.2 E 119 38 52.8
11	Fuqing	N 25 44 29 E 119 13 10	N 25 43 04.8 E 119 09 54				

tion on takeoffs and landings, the annual flow was extracted from airports all over the country from flight plans in 2013. Then the average daily flow between airports was obtained. Air routes for each aircraft depend on No. 1 Order of the Chinese Air Force^[18]. According to routes and daily flow between airports, the daily flow in each segment was confirmed, as shown in Table 2. According to Eqs. (7)—(9), the known information was used to calculate the conflict risk probability for each node, the total cost, and the network nonlinear coefficient, as shown in Table 3.

In the optimization module, the optimization model was developed for the G204, A470, B221, and A593 routes in ZSHA, and related parameters were set. According to Eq. (11), a shortest-path objective function was established. According to Eqs. (12)—(14), three constraint conditions were defined: avoiding PRDs, maintaining safety levels, and respecting boundary constraints.

To solve the process module, according to Section 2.1, a grid environment was established for ZSHA, as shown in Fig. 5. Then, as mentioned in Section 2.2, a search pattern was selected considering the relative positions of nodes. According to Section 2.3, aircraft search for the shortest path based on AACA; the dotted line in Fig. 5(b) represents the initial optimization path for A593. By increasing the number of grid cells, the optimal final path was found, as shown by the

solid line in Fig. 5(b). Then any constraint conditions on the optimal final path were checked. The constraints expressed in Eqs. (12), (14) were implemented in the process of executing the algorithm, and therefore the initially optimized ARN should satisfy Eq. (13). The conflict risk probability of the ARNN was less than $c_{\max} 1 \times 10^{-3}$ after calculation, as shown in Table 3. On the basis of these simulation results, the locations of the ARNNs before and after optimization are given in Table 1. A comparative diagram of the ARN before and after optimization is shown in Fig. 7. The aggregated indicators of the optimized ARN were evaluated and analyzed, as shown in Table 3.

Table 3 divides the optimization indicators into two categories: safety and economy. The former includes changes in the number of PRDs traversed, the number of nodes crossed, and the node hourly average potential flight conflict risk probabilities. This last includes changes in the ARN nonlinear coefficient, segment length, and operating cost. In the case of ZSHA, AACA successfully avoided nine PRDs which were traversed by routes G204, A470, B221, and A593. The number of intersecting nodes went from 5 to 2, a reduction of 60%. Under the conditions of the current flight flow, the flight conflict risk probability of the PiXian and LianJiang nodes was reduced by 24.321% and 74.179%, respectively, improving the safety level. The length of routes

Table 2 Segment and flow in ZSHA

Route	Segment/km	Length/ km	Flow value/ (vehicle · d ⁻¹)	Segment/km	Length/ km	Flow value/ (vehicle · d ⁻¹)
A593	EPGAM—Pixian	341	105	Pixian—Wuxi	364	15
	Wuxi—Pudong	146	15	Pudong—LAMEN	216	1
B221	Xuejiadao—POINT	541	1	POINT—ELAGO	76	1
	ELAGO—Andong	110	1	Andong—SUPER	43	1
	SUPER—Shengzhou	47	1	Shengzhou—Dongshan	207	49
	Dongshan—Lianjiang	201	26	—	—	—
A470	Pixian—Lishui	320	51	Lishui—Jianqiao	184	76
	Jianqiao—Tonglu	77	25	Tonglu—UGAGO	15	81
	UGAGO—Lianjiang	379	81	Lianjiang—Fuqing	56	107
	Fuqing—IKATA	316	42	—	—	—
G204	Jiuting—Andong	97	1	Andong—Shengzhou	83	1
	Shengzhou—UGAGO	112	3	UGAGO—Huangshan	136	1

Table 3 Optimization results

Feature	Index	Route	Current network	Optimized network	Change/%
Safety	Number of PRD		9	0	-100
	Number of cross nodes		5	2	-60
	Conflict risk probability	Pixian		6.554×10^{-4}	4.963×10^{-4}
Lianjiang			4.291×10^{-4}	1.108×10^{-4}	-74.179
Economy	ARN nonlinear coefficient		1.166	1.141	-2.144
		A593	1.067	1.049	-1.687
	Segment	A470	1.347	1.353	0.445
		Length/km	B221	1.225	1.235
	G204		428	343	-19.9
	Total length/km		4.067	3.980	-2.14
		A593	43.671	43.771	0.023
	Operation cost	A470	83.407	70.175	-15.864
		B221	16.186	15.288	-5.548
		G204	652	471	-27.761
Total cost		143.916	129.705	-9.875	

A470, A593, and B221 remained almost the same, but the length of route G204 was significantly reduced by 19.9%, resulting in a reduction of 2.14% in total route length. The nonlinear coefficient was reduced by 2.144% due to the shorter length. The cost of each route except for A593 was significantly reduced. The total cost of the four routes was reduced by 9.875%, improving the economic status of the ARN.

4 Conclusions

According to the relative position relationship of the starting and destination nodes, an AACA based on a grid model was selected to confirm the corresponding ant colony search mode. The optimization resulted in a decrease of 2.14% in total route length and a decrease of 9.875% in total operating cost, improving the operating economics of the ARN. The AACA optimization algorithm can reduce the number of search nodes, save computing time, improve optimization speed, and reduce the probability of singular segments. We will consider the interests of the airline from the perspective of airspace users, to establish a double ARNN optimization model, and to solve the optimization algorithm in future work.

Acknowledgements

This work was supported by the the Youth Science and Technology Innovation Fund (Science)(Nos. NS2014070, NS2014070).

References:

- [1] VU D, GILLES G, NICOLAON J, et al. Sector-Less air traffic management [C]// Air Traffic Management R&D Seminar. Santa Fe; AIAA, 2001; 1-7.
- [2] THOMAS R, PASCAL B. Shortest path in planar graph and air route network [C]// Proceedings of the 4th Eurocontrol Innovative Research Workshop & Exhibition. France; Eurocontrol, 2005; 1-10.
- [3] ZHOU J. Research of the airspace en route network based on the bi-level programming [D]. Nanjing: Nanjing University of Aeronautics and Astronautics, 2008. (in Chinese)
- [4] CAI K Q, ZHOU C. Optimization of the crossing waypoints in air route network [C]// Digital Avionics Systems Conference (DASC). USA; IEEE, 2010; 2. E. 3-1-2. E. 3-8.
- [5] XIAO M M, ZHANG J, CAI K Q, et al. Cooperative co-evolution with weighted random grouping for large-scale crossing waypoints locating in air route network [C]// Tools with Artificial Intelligence (IC-TAD). USA; IEEE, 2011; 215-222.
- [6] XIN Zhengwei. Research on air route network planning technology [D]. Nanjing: Nanjing University of Aeronautics and Astronautics, 2013. (in Chinese)
- [7] CHEN Cailong. Research on optimization method

- based on complex network for crossing waypoints location [D]. Hefei: University of Science and Technology of China, 2011. (in Chinese)
- [8] ZHAO Shuang. Research on national trunk air route network design [D]. Beijing: Beijing University of Aeronautics and Astronautics, 2008. (in Chinese)
- [9] WANG S J, GONG Y H. Research on air route network nodes optimization with avoiding the three areas [J]. Safety Science, 2014, 66: 9-18.
- [10] GUO H T, ZHU Q B, XU S J. Rapid-exploring random tree algorithm for path planning of robot based on grid method [J]. Journal of Nanjing Normal University (Engineering and Technology Edition), 2007, 7(2): 58-61.
- [11] ZHU B, ZHANG Y L. An ant colony algorithm based on grid method for mobile robot path planning [J]. Robot, 2005, 27(2): 132-136.
- [12] KAZUO S, SMITH J. Genetic algorithms for adaptive motion planning of an autonomous mobile robots [C]//Computational Intelligence in Robotics and Automation. USA: IEEE, 1997: 1-9.
- [13] ZHANG Y, WU C D, YU Q. Robot motion planning based on genetic algorithms [J]. Journal of Shenyang Arch And Civ Eng Univ (Natural Science), 2002, 18(4): 302-305.
- [14] HU Y L, ZHU L Z. The application research of genetic algorithm for the robot shortest path planning [J]. Machinery Design & Manufacture, 2002, 3(5): 109-111.
- [15] ZHANG M Y, HUANG H, HAO Z F, et al. Motion planning of autonomous mobile robot based on ant colony algorithm [J]. Journal of Environment Sciences, 2005, 25(1): 35-38.
- [16] Industry Administration Office of Civil Aviation Administration of China. AP-83-TM-2011-01, The safety assessment measures of air traffic management for the civil aviation [S]. Beijing: Civil Aviation Administration of China, 2011. (in Chinese)
- [17] Aeronautical Information Service Center of Bureau of Air Traffic Management of Civil Aviation Administration of China. National aeronautical information publication [S]. Beijing: Air Traffic Management of Civil Aviation Administration of China, 2014. (in Chinese)
- [18] The Chinese People's Liberation Army Headquarters. One regulation of flight control [S]. Beijing: The Chinese People's Liberation Army Headquarters, 2009. (in Chinese)

Dr. **Wang Shijing** is currently a lecture in College of Civil Aviation, Nanjing University of Aeronautics and Astronautics. She received her Ph. D. from College of Civil Aviation, Nanjing University of Aeronautics and Astronautics in 2011. Her main research interests are airspace planning and safety.

Ms. **Li Qingyun** is currently a postgraduate student in College of Civil Aviation, Nanjing University of Aeronautics and Astronautics. Her research interests include airspace planning, air route network planning and traffic engineering.

Ms. **Cao Xi** is currently a postgraduate student in College of Civil Aviation, Nanjing University of Aeronautics and Astronautics. Her research interests include network generated, network optimized and complex network.

Ms. **Li Haiyun** is currently a postgraduate student in College of Civil Aviation, Nanjing University of Aeronautics and Astronautics. Her research interests include network generated, network optimized and complex network.

(Executive Editor: Zhang Bei)